nature synthesis

Article

https://doi.org/10.1038/s44160-024-00484-x

# Enantioselective synthesis of a two-fold inherently chiral molecular nanographene

Received: 14 July 2023

Accepted: 17 January 2024

Published online: 22 February 2024

Check for updates

Manuel Buendía[1], Jesús M. Fernández-García[1], Josefina Perles[2], Salvatore Filippone[1] ✉ & Nazario Martín[1,3] ✉

The introduction and precise control of stereogenic elements in chemical structures is typically a challenging task. Most asymmetric methods require the presence of a heteroatom in the starting substrates acting as an anchor point for the successful transfer of chiral information. For this reason, compounds comprising only carbon atoms, such as optically active molecular nanographenes, are usually obtained as racemates, and isolated by chiral chromatographic separation. Here, we report an enantioselective strategy that uses three stereocontrolled synthetic steps to introduce and extend three different types of stereogenic elements, namely central, axial and helicoidal chirality, into a polycyclic aromatic structure. Thus, two chiral nanographene layers are covalently connected through a chiral triindane core. The final stereocontrolled graphitization Scholl reaction affords the formation of chiral nanographene units with remarkable enantiomeric excesses, high stereochemical stability and good chiroptical properties.

Chirality is an inherent property of objects whose importance in chemistry is widely recognized, as can be deduced from the considerable development of asymmetric synthesis[1–3]. The demand for optically active chemical compounds has expanded the realm of stereoselective chemical tools, while the requirements of the emergent scientific fields serve as a stimulus for further advances[4,5].

This applies to the broad interest in chirality that has emerged in fields such as materials science, nanoscience or organic electronics[4–8]. In this regard, organic compounds of interest must have highly π-conjugated structures and mainly consist of $sp^2$-hybridized carbon atoms or aromatic rings to ensure adequate optoelectronic properties, such as charge transport and/or light absorption and emission, to name a few[9,10]. However, the occurrence of chiroptical properties requires that these normally planar structures be deflected, bent or twisted, and that the originating stereogenic elements (axial chirality or less commonly planar chirality) can persist stably in the same system of π-conjugated carbon atoms[11–13]. For this reason, this type of chirality is notably more difficult to generate and control than central chirality: asymmetric synthesis provides only a limited number of methodologies available for preparing carbon-based π-conjugated chiral structures. In fact, most structures involve helicenes or arenes with limited π-extension, while, as far as we know, there is a lack of enantioselective methods for the non-racemic synthesis of inherently chiral (π-extended) nanographenes[12,14–20].

Chiral nanographenes consist of arrays of fused aromatic rings that are forced to diverge from their natural planar geometry into a helical substructure because of strain stemming from stereogenic defects[21]. The asymmetrical folding of these large aromatic surfaces is such a difficult task that optically active molecular nanographenes have so far been mostly obtained after expensive and time-consuming high-performance liquid chromatography (HPLC) separations[22]. To our knowledge, there are only a few examples of optically active nanographenes that have been directly synthesized[23–25]. In all these examples, chirality stems from the stereogenic axes already present in the starting material without introducing any further stereogenic element.

The enantioselective synthesis of all-carbon compounds, and thus of nanographenes, faces another difficulty: most enantioselective methods rely on the presence of heteroatoms in the reagents, which act as a steering group on which the chiral information pivots and,

[1]Departamento de Química Orgánica I, Facultad de Ciencias Químicas, Universidad Complutense de Madrid, Ciudad Universitaria s/n, Madrid, Spain. [2]Laboratorio DRX Monocristal, SIdI, Universidad Autónoma de Madrid, Madrid, Spain. [3]IMDEA-Nanociencia, Campus de Cantoblanco, Madrid, Spain. ✉e-mail: salvatore.filippone@ucm.es; nazmar@ucm.es

https://doi.org/10.1038/s44160-024-00484-x

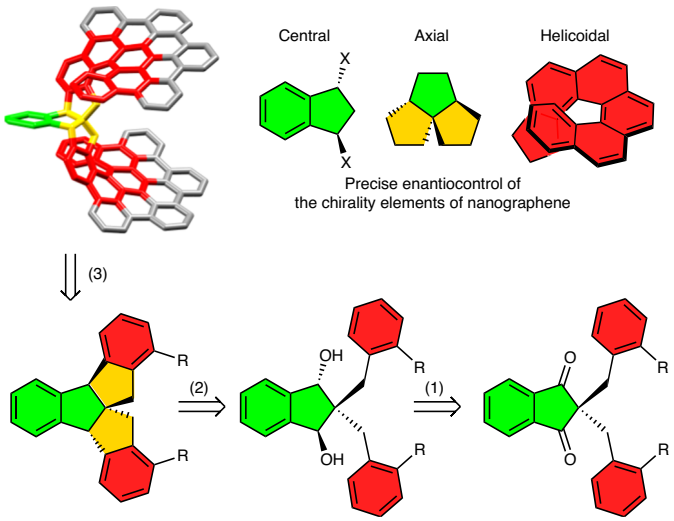


**Fig. 1 | Retrosynthetic scheme for the enantioselective synthesis of an all-carbon nanographene.** A two-fold inherently chiral nanographene has been achieved involving three types of chiral elements, namely central, axial and helicoidal, in the backbone structure (top). The reverse transformations involve: (3) enantiospecific Scholl oxidation coupling (stereocontrolled graphitization); (2) enantiospecific benzylic substitution (ring closing with heteroatom removal) and (1) introduction of chiral information (stereodirecting detachable heteroatom) (bottom).

eventually, they persist in the products. In the case of nanographenes, this entails substantial changes in their optoelectronic properties.

Herein, we present an enantioselective synthesis of an inherently chiral bilayer nanographene by precise enantiocontrol of an extended pattern of stereogenic elements generated in the molecular core. Therefore, instead of peripheral chirality, central, axial (spiro group) and helicoidal chirality have been successfully combined along the skeleton to achieve a stable, rigid and adequately twisted structure (Fig. 1). It is important to note that the nanographenic substructures with six *ortho*-fused rings in a helical arrangement has been achieved asymmetrically without the need to elongate the synthetic pathway with further steps with respect to the racemic route. Instead, we introduced the appropriate chiral information simply by carrying out precise enantiocontrol in three key steps of the synthesis: enantioselective ketone reduction followed by enantiospecific benzylic substitution with removal of the heteroatom. Finally, an enantiospecific Scholl reaction allowed directional bending of the π-conjugated system, thus achieving an inherently chiral double-layer nanographene (Fig. 1).

Our design is based on the generation of a spiranic unit with axial chirality (yellow substructure in Fig. 1). We planned an angular centrotriindane (yellow-green structure in Fig. 1)[26] as a stair landing between two spiral staircases with the same handedness (red helicene substructure, Fig. 1), which would allow extending the helicoidal motif along the skeleton of the molecular nanographene. Angular centrotriindane has previously been synthesized only in racemic form[27]. Therefore, its asymmetric synthesis has been challenging and demonstrates the usefulness of our three-stage strategy for the enantioselective preparation of heteroatom-free spiro compounds.

For the racemic synthesis (Fig. 2, route 1) of the centrotriindane-based nanographene, we were inspired by the work of Kuck[27]. Thus, starting from 1,3-indandione, after double benzylation, Sonogashira cross-coupling reaction and further [4+2] cycloaddition reaction with cyclopentadienone **4**, we obtained indandione **5** endowed with two hexarylbenzene units. The reduction with $LiAlH_4$ proceeded with excellent diastereoselectivity, yielding racemic diol **6** in a *trans* configuration, while *meso*-**6** was not found.

At the next stage, the helicene substructure that will impart curvature to the final nanographene begins to form. Thus, we carried out a twofold intramolecular Friedel–Crafts reaction with the closest phenyl group of the polyarylbenzene moiety for ring closing of the six *ortho*-fused rings. Moreover, we took advantage of this double five-membered ring formation to remove the two oxygen atoms. Instead of polyphosphoric acid previously used by Kuck[27], we used triphenylphosphine ditriflate (Hendrickson reagent)[28] to promote the nucleophilic substitution of the two hydroxy benzylic groups by the closest aryl group of the polyarylbenzene (Fig. 2, route 1).

During this step, a second (axial) chirality element is generated without affording a stereoisomeric mixture (Fig. 2). Indeed, the spiro system in centrotriindane **7** is formed diastereoselectively to avoid *trans* junctions in the fused five-membered rings and, therefore, its configuration stems from the configuration of the starting stereogenic centres (Fig. 2). Thus, a sole diastereomer **7** is formed as a pair of enantiomers with $R,R,R_a$ or $S,S,S_a$ configuration in the two stereogenic centres and in the axially chiral spiro carbon, respectively (Fig. 2, route 1). The structure of **7** has been confirmed by X-ray analysis of a racemic sample (Supplementary Fig. 8).

Finally, racemic mixture **7** was submitted to dehydrogenative Scholl reaction conditions, affording molecular nanographene **1** featuring two connected helicoidal substructures of [5+1] rings. Despite the generation of two other chiral elements, the reaction took place diastereoselectively, affording a sole nanographene **1** as a pair of enantiomers with $(S,S,S_a,M,M)$-**1** and $(R,R,R_a,P,P)$-**1** configurations. The final structure, which has been assigned by NMR spectroscopic analysis, was confirmed by X-ray diffraction of a racemic sample (Supplementary Fig. 14). To our delight, it could be visualized as a double helicene structure with the same handedness connected by an indane moiety.

On obtaining the racemic nanographene **1**, we sought to find a step in this synthesis that could be stereoselectively directed and that would allow us to introduce the necessary chiral information. Thus, we turned our attention to the enantioselective reduction of ketones, which has proved to be an efficient way to form chiral alcohols. However, the enantioselective reduction of indandione **5** is not a trivial process because it involves a twofold asymmetric reduction of two neighbouring and electronically connected carbonyl groups along with a quaternary carbon in the α position, which hinders both reduction and stereocontrol processes. In fact, many of our attempts based on the reported asymmetric hydrogenation methods were unsuccessful in reducing 1,3-indandione (Supplementary Table 1)[29–32]. An exception was the Corey–Bakshi–Shibata reduction, which is based on the use of borane in the presence of a chiral oxazaborolidine[33,34]. However, commonly used catalysts, such as (*S*)-*ortho*-tolyl- or methyl-oxazaborolidine instead of *trans*-**6** diol, yielded *cis*-**6** diol, which, being a *meso* compound, is useless for performing an enantioselective pathway.

Given the ability of borane to reduce 1,3-indandione and the ease of forming these catalysts from inexpensive and readily available derivatives, such as prolinol and boronic acids, we screened other oxazaborolidines. To our delight, we found that *p*-methoxyphenyl oxazaborolidine (pMPOAB), used in large excess, was able to direct the asymmetric reduction towards both *trans* diols in around 70:30 [*trans*-**6**:*meso*-**6**] diastereomeric ratio and as sole enantiomer (enantiomeric excess (e.e.) ≥ 97%; Fig. 2, routes 2 and 3). We hypothesized that the observed low diastereoselectivity is a consequence of the second addition, now occurring on a more reactive chiral substrate, which, eventually, directs the reduction to the opposite face with respect to that of the catalyst, thus resulting in the *meso* compound. The presence of electron-donating groups, such as methoxy, in the arene should favour the interaction of the arene π system with the empty boron $p_z$ orbital, thus enabling a larger amount of complex formation by a stronger interaction between the oxazaborolidine nitrogen and the borane molecule.

https://doi.org/10.1038/s44160-024-00484-x

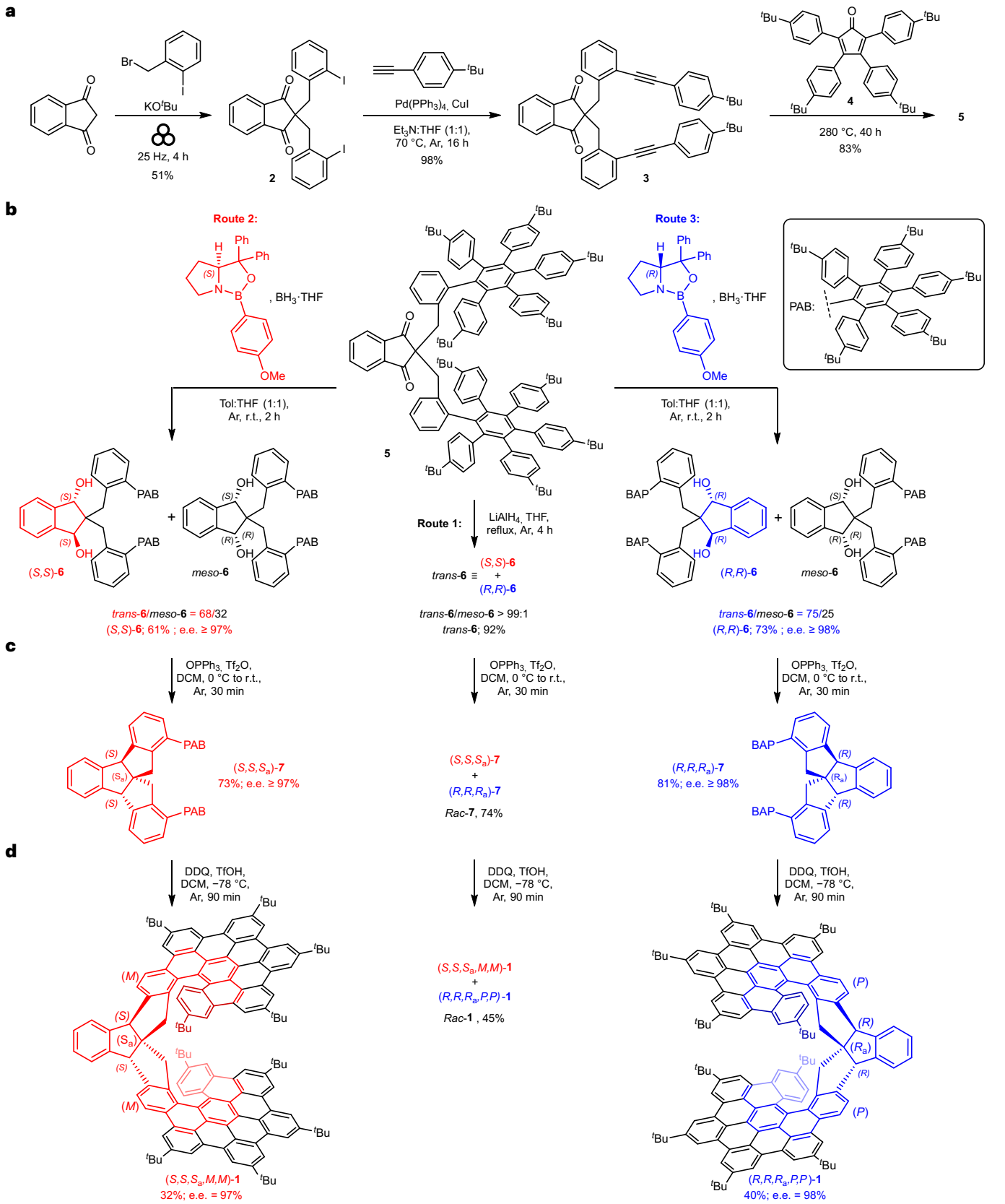


**Fig. 2 | Sequential steps for the synthesis of centrotriindane-based nanographene 1. a**, Preparation of bis-hexarylbenzene starting material. **b**, Introduction of chiral information by the generation of two stereogenic centres; the reduction of indandione **5** using $LiAlH_4$ (racemic, route 1) affords diastereoselectively diol *trans*-**6** as a racemic mixture, while Corey–Bakshi–Shibata reduction with borane and (*S*)-oxazaborolidine (based on natural prolinol, route 2) or (*R*)-oxazaborolidine (route 3) affords indandiol (*S*,*S*)-**6** or (*R*,*R*)-**6**, respectively. **c**, Enantiospecific benzylic substitution with heteroatom removal; both racemic as well as enantiopure indandiols **6** undergo an enantiospecific ring-closing reaction. **d**, Enantiospecific Scholl oxidation gives rise to a stereocontrolled graphitization, maintaining the chiral information of triindane **7** starting material. PAB, penta(*p*-*tert*-butylphenyl)benzene; DCM, dichloromethane; DDQ, 2,3-dichloro-5,6-dicyano-*p*-benzoquinone; r.t., room temperature.

https://doi.org/10.1038/s44160-024-00484-x

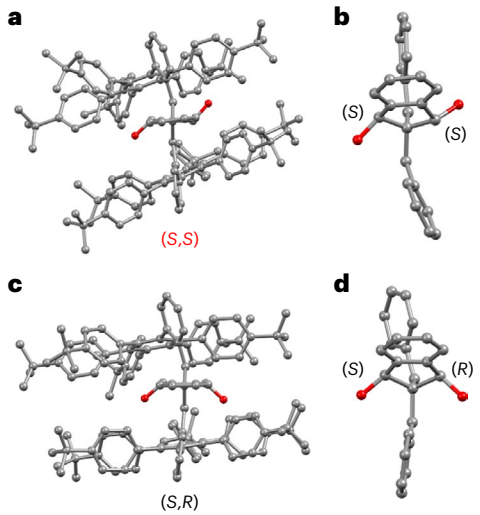


**Fig. 3 | Single-crystal X-ray structures for compound 6. a**, X-ray structure of (*S*,*S*)-**6** obtained with chiral oxazaborolidine (*S*)-*p*MPOAB. **b**, Simplified structure of 1,3-indandiol core of (*S*,*S*)-**6**. **c**, X-ray structure of *meso*-**6**. **d**, Simplified structure of 1,3-indandiol core of *meso*-**6**.

In this way, both enantiomers have been easily prepared. The configuration (*S*,*S*)-**6** was assigned to the enantiomer obtained when (*S*)-oxazaborolidine (based on natural prolinol) was used. This assignment has been carried out on the basis of X-ray diffraction analysis (Fig. 3a and Supplementary Fig. 2), as well as on the sense of the asymmetric induction (*Re* face) reported in the literature[33,34].

Once generated, the new stereocentres must be preserved in the next synthetic step, where the same benzylic stereogenic carbon atoms are involved in the ring closure by nucleophilic substitution of the two hydroxyl groups. This $S_N1$ reaction takes place through the formation of a stabilized benzylic carbocation with complete racemization. Much effort has been devoted to controlling the stereochemistry of such carbon atoms. However, as far as we know, it has only been achieved in a few transformations, and never when a carbon atom is engaged as a nucleophile in the reaction[35–37].

Thus, we turned our attention to a Friedel–Crafts-type benzylation of arenes mediated by triphenylphosphonium anhydride trifluoromethanesulfonate (Hendrickson reagent)[28]. The synthetic challenge was to ascertain whether such a reagent would allow enantiospecific cyclization via carbon–carbon bond generation in a Mitsunobu-type reaction without loss of chiral information.

Each enantiomer was further submitted to intramolecular Friedel–Crafts reaction with the benzylic hydroxyl group, to afford two five-membered rings along with the generation of another chiral unit in the new spiro system (Fig. 2, routes 2 and 3). Remarkably, this twofold cyclization, where two new C–C carbon bonds are formed, was fully enantiospecific. Thus, triindanes (*R*,*R*,$R_a$)-**7** and (*S*,*S*,$S_a$)-**7** were obtained from diols (*R*,*R*)-**6** and (*S*,*S*)-**6**, respectively, in both cases with e.e. > 97% (Fig. 2, routes 2 and 3).

These exceptional e.e. values can be explained either by the presence of a second stereogenic centre in the proximity, or by the ability of the triphenylphosphonium salt (Hendrickson reagent) to prevent the formation of benzyl carbocations in the reaction with diols **6**.

On one hand, no loss of optical purity is observed, even when a weak nucleophile, such as the arene group, is involved. On the other hand, we observed complete inversion of configuration at the substituted carbons, which could be accounted for by a Mitsunobu-type $S_N2$ substitution reaction. The absolute configuration of the two stereogenic carbons involved in the substitution has been confirmed by X-ray analysis of the final nanographenes. The fact that the configuration of these carbons does not apparently change in the presence of a configuration inversion is due to the formalisms of the Cahn–Ingold–Prelog priority rules.

It is worth noting that this methodology enables the asymmetric synthesis of two important classes of chiral organic compounds, namely spiro compounds[38] and hexarylbenzenes (HABs), with their less-common features of 'toroidal interaction' owing to the electronic coupling of π-orbitals of peripheral aromatic rings[39].

As expected, X-ray analysis of HABs (*S*,*S*)-**6** and *rac*-**7** (Supplementary Figs. 2, 6 and 8) reveals the presence of propeller-shape structures featuring radial aromatic blades twisted with respect to the central benzene core. Interestingly, the resulting stereogenic elements do not appear to generate a sole propeller chirality in the crystals. In fact, the two HABs present in each molecule exhibit both clockwise and anticlockwise handedness, even in (*S*,*S*)-**6** chiral crystals (Fig. 3 and Supplementary Figs. 2, 6 and 8). The stereoselectively generated enantiomers of the hexarylbenzenes **7** were subjected to dehydrogenative oxidation Scholl reaction conditions, affording the final nanographene **1**, which was asymmetrically curved. Indeed, the presence of the three chiral elements directed the intramolecular oxidative coupling, generating, in an enantiospecific manner, two helicene substructures formed by six *ortho*-fused rings, which ensure a stable configuration. Thus (*R*,*R*,$R_a$,*P*,*P*)-**1** and (*S*,*S*,$S_a$,*M*,*M*)-**1** were obtained from (*R*,*R*,$R_a$)-**7** and (*S*,*S*,$S_a$)-**7**, respectively, with enantiomeric excess values surpassing 97%, thus confirming the complete enantiospecificity of the process (Fig. 2, routes 2 and 3).

Our design enables the enantioselective synthesis of a molecular nanographene in a very high enantiomeric excess. This experimental finding can be rationalized considering that the chiral information introduced in the indandiol (*S*,*S*)-**6** is maintained during the two-fold substitution of the OH groups in the ring-closing process at the benzylic carbon atoms. Although other mechanisms cannot be ruled out, a possible mechanism involves the nucleophilic attack of the arene in the Friedel–Crafts reaction occurring on the opposite side to the outgoing phosphine oxide group, thus preventing the formation of a benzyl carbocation in a Mitsunobu-type process (Fig. 4a). X-ray crystallographic analysis of the enantiomerically pure nanographene **1** confirms the inversion of configuration at the two benzylic carbon atoms (Fig. 5a).

Regarding the stereoselective formation of the two helical substructures that feature the same handedness, *M*,*M* or *P*,*P*, this stereochemical outcome depends on which of the two benzenes (Fig. 4b, orange- or blue-labelled phenyl group) binds the adjacent indene group. If we consider the polyarylbenzene unit in such a way that the peripheral aryl groups are orthogonal to the central benzene, the nucleophilic attack of the orange-labelled aryl on the left (Fig. 4b) to the *Si* face of the indene group in (*S*,*S*,$S_a$)-**7** is favoured, while the *Re* face is shielded from the starting indane moiety (Fig. 4b). Thus, a double *M* configuration is generated in the two nanographenic layers, while the (*S*,*S*,$S_a$,*P*,*P*)-**1** stereoisomer has not been observed.

Two crystal structures were solved by single-crystal X-ray diffraction for compound **1**. The enantiopure crystal contains two (*S*,*S*,$S_a$,*M*,*M*)-**1** molecules in the asymmetric unit, with small conformational differences (Supplementary Figs. 11 and 15). In these molecules, the two hexabenzocoronene (HBC) fragments are highly twisted, with the shortest distance between centroids from rings in opposite layers of 7.743 Å (between the distal ones). The packing of the molecules in the crystal is achieved by C–H···π and π···π interactions between neighbours in the [010] direction (Fig. 5a). In the case of the racemic crystal of *rac*-**1** (Fig. 5b), containing both (*S*,*S*,$S_a$,*M*,*M*) and (*R*,*R*,$R_a$,*P*,*P*) molecules, the asymmetric unit contains half a molecule, as the molecule is located around a rotation two-fold axis. The conformation of the molecule is very similar to the one found in the enantiopure crystal (Supplementary Fig. 15). However, the overall structure is more compact due to more efficient packing of the alternating enantiomers within a column, owing to the better overlap of the rings at the end of

https://doi.org/10.1038/s44160-024-00484-x

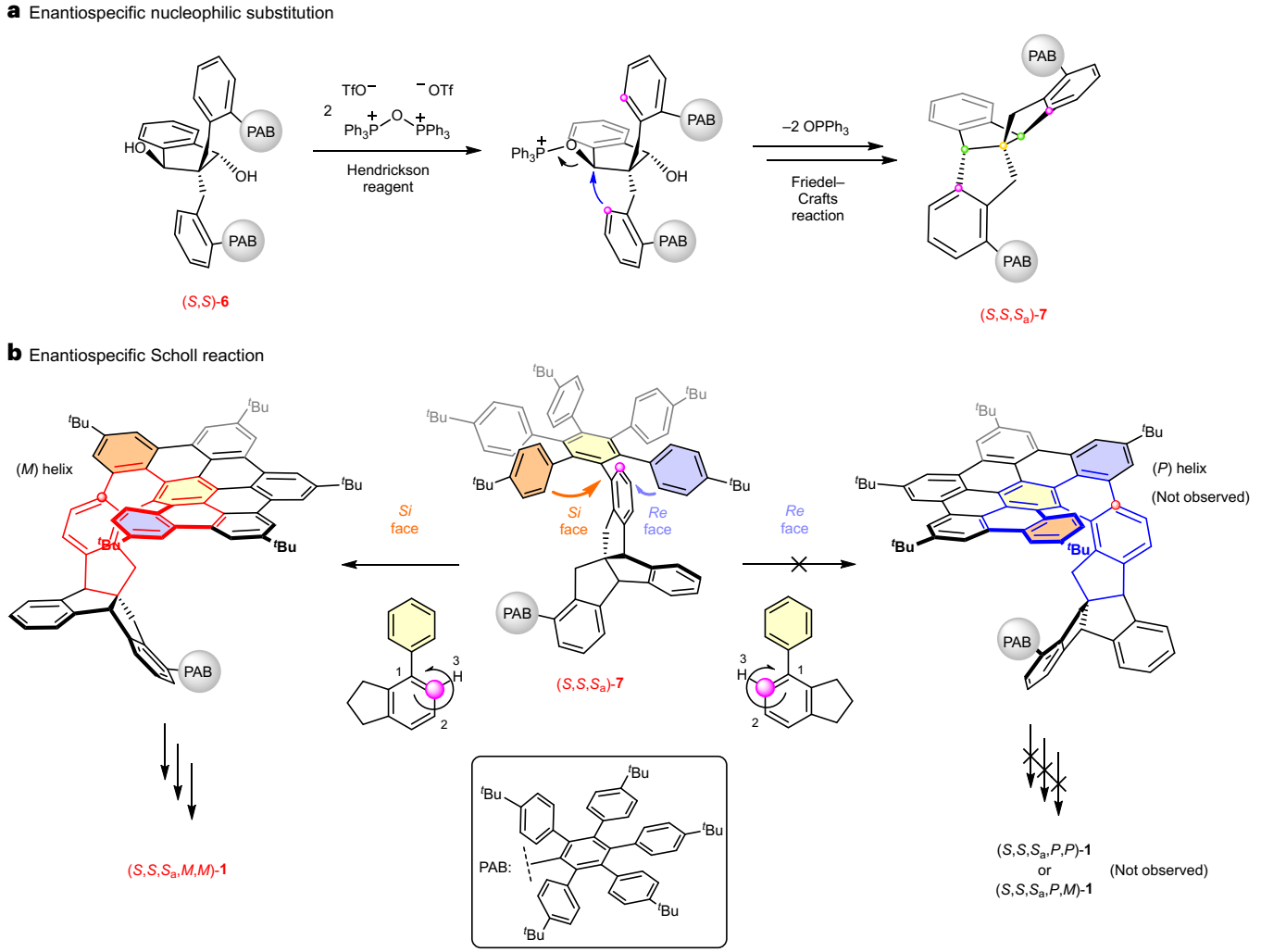


**Fig. 4 | Synthetic steps transferring chiral information. a**, A Mitsunobu-like $S_N2$ reaction is a plausible mechanism for the observed stereochemical results in the Hendrickson reaction for (*S*,*S*)-**6**. As shown by X-ray crystallographic analysis of (*S*,*S*,$S_a$,*M*,*M*)-**1**, there is an inversion of configuration for the two stereogenic centres of the indane moiety (green). **b**, A plausible mechanism for the observed enantiospecificity in the Scholl reaction for (*S*,*S*,$S_a$)-**7** is based on the effect of the indane closest to the reaction centre hindering the nucleophilic attack of the adjacent phenyl group (purple) from the *Re* face.

the nanographene layers, yielding shorter distances between adjacent molecules (Supplementary Figs. 14 and 16).

Absorption and emission spectroscopy was performed to characterize the electronic properties of **1**. These spectra have been compared to those of the hexa-*tert*-butyl-hexa-*peri*-hexabenzocoronene (*t*-BuHBC) as a reference. Thus, the absorption spectrum of **1** resembles that of *t*-BuHBC, having the highest band at 361 nm, with a shoulder at 323 nm. In the visible region, two bands at 418 nm and 467 nm of lower intensity are observed. The emission spectrum of **1** shows a maximum at 469 nm, and two bands at 500 nm and 534 nm as the main features. According to the emission wavelength observed, nanographene **1** emits a vivid blue fluorescence as a consequence of the electron quantum confinement in these systems (Fig. 6a).

Having obtained the absolute configuration by X-ray spectroscopic analysis, we can associate the chiroptical responses in absorption and emission to the absolute configuration of each enantiomer. Moreover, the chiroptical behaviour is similar to that observed for related structures based on double [6]helicenes[40–42].

The electronic circular dichroism of both enantiomers shows the expected mirror image shape, with two main bisignate signals at 328 and 375 nm (Fig. 6b). At larger wavelengths, (*R*,*R*,$R_a$,*P*,*P*)-**1** shows a low-intensity peak with negative sign at 470 nm and a positive peak of medium intensity at 420 nm. With regard to the circularly polarized luminescence spectra, the sign is the same as the 470 nm peak of the electronic circular dichroism spectra: positive for (*S*,*S*,$S_a$,*M*,*M*)-**1** and negative for (*R*,*R*,$R_a$,*P*,*P*)-**1** with a maximum at 474 nm and a $g_{lum} = 1.9 \times 10^{-3}$ (Fig. 6c). Circularly polarized luminescence brightness ($B_{CPL}$) was also calculated at an excitation wavelength of 373 nm, resulting in $B_{CPL} = 16.7\ M^{-1}cm^{-1}$. These experimental values are in the same range as that for other related systems[43–48].

To sum up, we have reported the enantioselective synthesis of a two-fold chiral molecular nanographene obtained at will in both enantiomeric forms, namely (*R*,*R*,$R_a$,*P*,*P*)-**1** and (*S*,*S*,$S_a$,*M*,*M*)-**1**, without employing chiral starting materials or expensive and time-consuming chiral HPLC separation. Both enantiomerically pure nanographenes have been obtained by a precise enantiocontrol from a sequential introduction of stereogenic elements generated along their respective synthesis, namely central, axial (spiro group) and helicoidal chirality. Although, the chiral information is introduced using an oxygen atom as steering group in a double enantioselective ketone reduction, heteroatom removal has been exploited in the subsequent ring-closing synthetic step. Indeed, a quite uncommon enantiospecific double substitution of two OH groups at chiral benzylic carbon atoms has been carried out in a Mitsunobu-type reaction with a less-explored carbon-based aromatic nucleophile. An enantiopure triindane spiro compound has thus been obtained with complete inversion of configuration at

https://doi.org/10.1038/s44160-024-00484-x

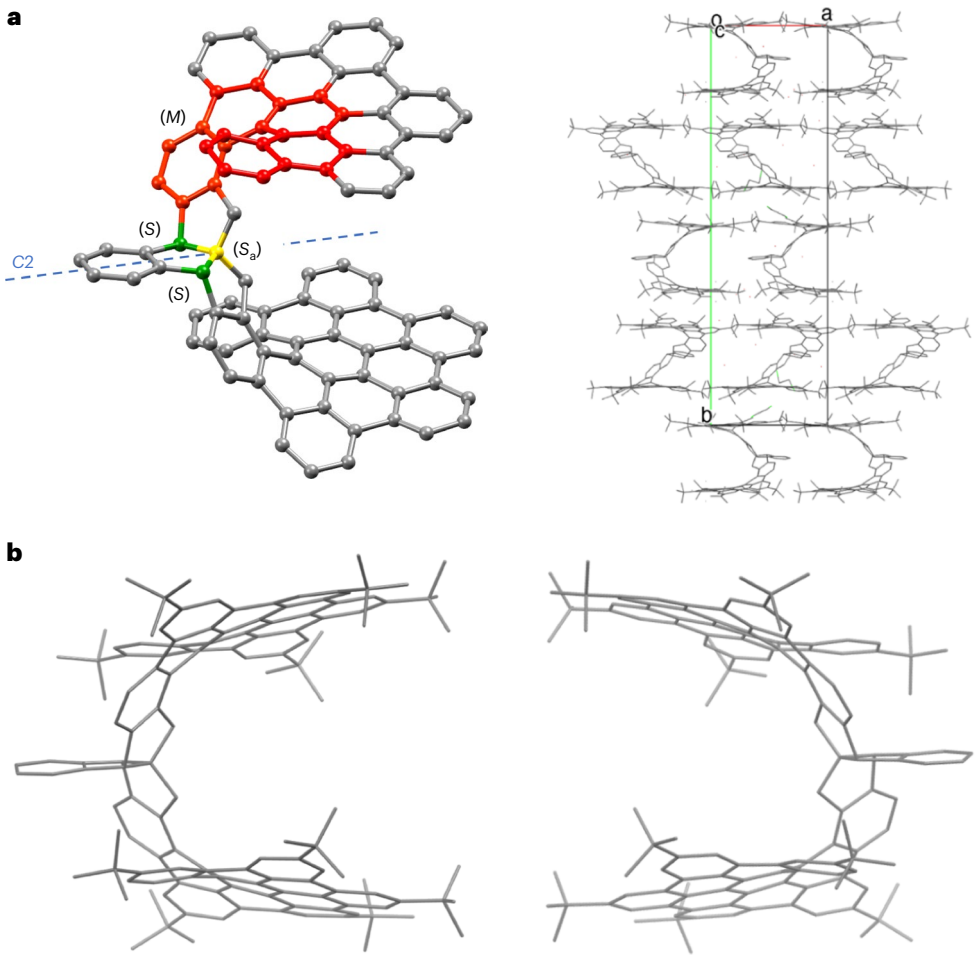


**Fig. 5 | Single-crystal X-ray structures for compound 1. a**, Molecular structure and packing of enantiopure nanographene (*S*,*S*,*S*$_a$,*M*,*M*)-**1**. **b**, Enantiomers present in the crystal structure of *Rac*-**1** (left, (*R*,*R*,*R*$_a$,*P*,*P*); right, (*S*,*S*,*S*$_a$,*M*,*M*)).

the benzylic carbon atoms. The chiral information has been retained up to the final molecular nanographene **1**, thanks to a complete enantiospecific graphitization Scholl reaction, where the formation of six *ortho*-fused rings introduces the last helicoidal stereogenic element directly into the core of the extended π-conjugated system.

As a result of this inherent chirality stemming from the nanographene core, both enantioselectively obtained enantiomers (*R*,*R*,*R*$_a$,*P*,*P*)-**1** and (*S*,*S*,*S*$_a$,*M*,*M*)-**1** exhibit intense specular circular dichroism. Each circular dichroism spectrum has been unambiguously assigned to each enantiomer as a result of full characterization by X-ray diffraction analysis from a suitable single crystal of the (*S*,*S*,*S*$_a$,*M*,*M*)-**1** enantiomer.

This approach is a useful synthetic strategy that paves the way to access other chiral heteroatom-free hydrocarbons, such as spiro compounds, and, in particular, enables the enantioselective synthesis of chiral all-carbon molecular nanographenes.

## Methods

### General procedure for the synthesis of Corey–Bakshi–Shibata pMPOAB oxazaborolidine

In a round-bottom flask provided with a magnetic stir bar, (*S*)-(−) or (*R*)-(+) α,α-diphenyl-2-pyrrolidinemethanol (1 equiv., ~0.089 M) and 4-methoxyphenylboronic acid (1 equiv., ~0.089 M) and anhydrous toluene were placed under an Ar atmosphere. A 50 ml addition funnel provided with activated 4 Å molecular sieves was placed in the neck of the flask, acting as a Soxhlet extractor to dry out water from the system. The mixture was stirred and heated to reflux under an Ar atmosphere overnight (~16 h). The solvent was reduced to concentrate the catalyst solution to ~3 ml (~0.75 M) and stored in an Ar atmosphere before using.

### General procedure for the enantioselective reduction of 1,3-indandione derivative (5) with Corey–Bakshi–Shibata pMPOAB oxazaborolidines

To a solution of either (*S*)-(−) or (*R*)-(+) *p*MPOAB in toluene (~0.75 M), a solution of $BH_3$·THF in THF (1 equiv.) was added at room temperature under an Ar atmosphere. The mixture was stirred for 30 min to form the catalytic complex, to which the 1,3-indandione derivative **5** was added (0.04 equiv.). The reaction was stirred at room temperature upon completion, cooled in an ice bath and diluted with diethyl ether before adding water in a dropwise manner to quench it. The mixture was then washed with a HCl 0.1 M solution and water. The organic phase was dried with $MgSO_4$ and the solvent removed under reduced pressure. The crude—a mixture of two diastereomers—was purified by silica gel column chromatography using hexane:DCM (5:1) as eluent.

### General procedure for the enantiospecific ring-closing reaction

The Hendrickson salt was prepared in a regular dried vial provided with a magnetic stir bar, where freshly distilled trifluoromethanesulfonic anhydride (1 equiv.) was added to a solution of triphenylphosphine oxide in anhydrous DCM (2 equiv., ~0.17 M) at 0 °C. The mixture was stirred for 20 min, upon complete formation of a white precipitate. The white precipitate was quickly added to a solution of a *trans*-1,3-indandiol derivative (*trans*-**6**, (*S*,*S*)-**6** or (*R*,*R*)-**6**) in anhydrous DCM

https://doi.org/10.1038/s44160-024-00484-x

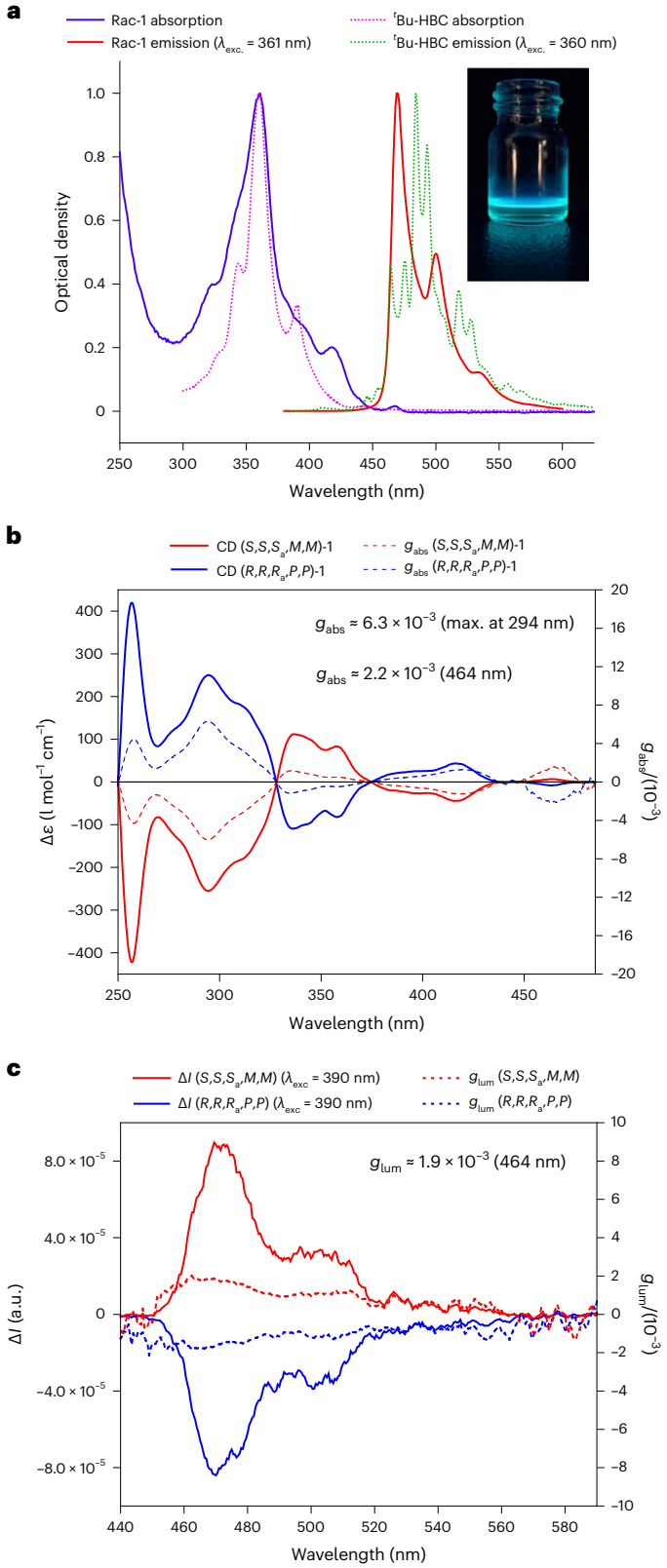


**Fig. 6 | Optical and chiroptical spectra of nanographene 1.** **a**, Normalized absorption and emission spectra for nanographene **1** compared to *t*-BuHBC ($CHCl_3$, 20 °C) (inset: fluorescence of **1** solution in $CHCl_3$ under a 365 nm lamp). **b**, Circular dichroism absorption spectra (solid lines) for both enantiomers (*S*,*S*,$S_a$,*M*,*M*)-**1** (in red) and (*R*,*R*,$R_a$,*P*,*P*)-**1** (in blue) ($CHCl_3$, 20 °C, 10 µM) and absorptive dissymmetry factor ($g_{abs}$) (dashed lines). **c**, Circularly polarized luminescence spectra (solid lines) of (*S*,*S*,$S_a$,*M*,*M*)-**1** (in red) and (*R*,*R*,$R_a$,*P*,*P*)-**1** (in blue) and luminescence dissymmetry factor ($g_{lum}$) (dashed lines) ($\lambda_{exc}$ = 390 nm, $CHCl_3$, 20 °C, ~1 µM).

(0.5 equiv., ~0.02 M), also at 0 °C under Ar atmosphere, stirring the reaction mixture for 30 min. The reaction was then quenched with a saturated solution of $NaHCO_3$, diluted in DCM and washed with more $NaHCO_3$ solution and water. The organic phase was dried with $MgSO_4$ and the solvent removed under reduced pressure. The crude was purified by silica gel column chromatography using hexane:DCM (5:1) as eluent.

### General procedure for the enantiospecific Scholl reaction

To a solution of a triindane derivative (*rac*-**7**, (*S*,*S*,$S_a$)-**7** or (*R*,*R*,$R_a$)-**7**) in anhydrous DCM (1 equiv., ~0.7 mM) and DDQ (11 equiv.) at −78 °C under Ar atmosphere, trifluoromethanesulfonic acid was added (110 equiv.). The mixture was stirred for 90 min at −78 °C with an Ar flow. The reaction was then quenched with a saturated solution of $NaHCO_3$, warmed up to room temperature and washed with more $NaHCO_3$ solution and water. The organic phase was dried with $MgSO_4$ and the solvent removed under reduced pressure. The diastereoselectivity of the reaction was monitored by $^1$H NMR of the crude. Chiral bilayer nanographene derivatives (*rac*-**1**, (*S*,*S*,$S_a$,*M*,*M*)-**1** or (*R*,*R*,$R_a$,*P*,*P*)-**1**) were purified by silica gel column chromatography using hexane:DCM (10:1) as eluent. Enantiomeric excesses of (*S*,*S*,$S_a$,*M*,*M*)-**1** or (*R*,*R*,$R_a$,*P*,*P*)-**1** were monitored through chiral HPLC. HPLC analyses were performed on a JASCO LC-4000 series equipped with a UV–visible and CD detector. Control method required (*R*,*R*) Whelk-O 2 (5 µm, 25 cm × 4.6 mm internal diameter) as HPLC analytical column/chiral stationary phase; Hex:THF:IPA (98:1:1) as mobile phase; 0.5 ml $min^{-1}$ flow; a 40 °C oven temperature; and wavelength detector was set at $\lambda$ = 254 nm.

## Data availability

All the data generated or analysed that support the findings of this study are included in this article and its Supplementary Information. Crystallographic data for the structures reported in this Article have been deposited at the Cambridge Crystallographic Data Centre, under deposition numbers CCDC 2278583 ((*S*,*S*)-**6**), 2278584 (*meso*-**6**), 2278585 (*rac*-**7**), 2278586 ((*S*,*S*,$S_a$,*M*,*M*)-**1**) and 2278587 (*rac*-**1**). Copies of the data can be obtained free of charge via https://www.ccdc.cam.ac.uk/structures/. Source data are provided with this paper.

## References


1. Akiyama, T. & Ojima, I. *Catalytic Asymmetric Synthesis*. John Wiley & Sons, 2022.
2. Cheng, J. K., Xiang, S.-H., Li, S., Ye, L. & Tan, B. Recent advances in catalytic asymmetric construction of atropisomers. *Chem. Rev.* **121**, 4805–4902 (2021).
3. Xiang, S.-H. & Tan, B. Advances in asymmetric organocatalysis over the last 10 years. *Nat. Commun.* **11**, 3786 (2020).
4. Wang, Y., Xu, J., Wang, Y. & Chen, H. Emerging chirality in nanoscience. *Chem. Soc. Rev.* **42**, 2930–2962 (2013).
5. Kuang, H., Xu, C. & Tang, Z. Emerging chiral materials. *Adv. Mater.* **32**, e2005110 (2020).
6. Brandt, J. R., Salerno, F. & Fuchter, M. J. The added value of small-molecule chirality in technological applications. *Nat. Rev. Chem.* **1**, 0045 (2017).
7. Fernandez-Garcia, J. M., Evans, P. J., Filippone, S., Herranz, M. A. & Martin, N. Chiral molecular carbon nanostructures. *Acc. Chem. Res.* **52**, 1565–1574 (2019).
8. Kotov, N. A., Liz-Marzán, L. M. & Weiss, P. S. Chiral nanostructures: new twists. *ACS Nano* **15**, 12457–12460 (2021).
9. Ostroverkhova, O. Organic optoelectronic materials: mechanisms and applications. *Chem. Rev.* **116**, 13279–13412 (2016).
10. Forrest, S. R. & Thompson, M. E. Introduction: organic electronics and optoelectronics. *Chem. Rev.* **107**, 923–925 (2007).
11. Bedi, A. & Gidron, O. The consequences of twisting nanocarbons: lessons from tethered twisted acenes. *Acc. Chem. Res.* **52**, 2482–2490 (2019).

12. Rickhaus, M., Mayor, M. & Juricek, M. Chirality in curved polyaromatic systems. *Chem. Soc. Rev.* **46**, 1643–1660 (2017).
13. Rickhaus, M., Mayor, M. & Juricek, M. Strain-induced helical chirality in polyaromatic systems. *Chem. Soc. Rev.* **45**, 1542–1556 (2016).
14. Link, A. & Sparr, C. Stereoselective arene formation. *Chem. Soc. Rev.* **47**, 3804–3815 (2018).
15. Stara, I. G. & Stary, I. Helically chiral aromatics: the synthesis of helicenes by [2+2+2] cycloisomerization of π-electron systems. *Acc. Chem. Res.* **53**, 144–158 (2020).
16. Izquierdo-Garcia, P. et al. Helical bilayer nanographenes: impact of the helicene length on the structural, electrochemical, photophysical, and chiroptical properties. *J. Am. Chem. Soc.* **145**, 11599–11610 (2023).
17. Redero, P. et al. Enantioselective synthesis of 1-aryl benzo[5] helicenes using BINOL-derived cationic phosphonites as ancillary ligands. *Angew. Chem. Int. Ed. Engl.* **59**, 23527–23531 (2020).
18. Zhang, F., Michail, E., Saal, F., Krause, A. M. & Ravat, P. Stereospecific synthesis and photophysical properties of propeller-shaped $C_{90}H_{48}$ PAH. *Chem. Eur. J.* **25**, 16241–16245 (2019).
19. Roy, M. et al. Stereoselective syntheses, structures, and properties of extremely distorted chiral nanographenes embedding hextuple helicenes. *Angew. Chem. Int. Ed. Engl.* **59**, 3264–3271 (2020).
20. Yubuta, A. et al. Enantioselective synthesis of triple helicenes by cross-cyclotrimerization of a helicenyl aryne and alkynes via dynamic kinetic resolution. *J. Am. Chem. Soc.* **142**, 10025–10033 (2020).
21. Fernandez-Garcia, J. M., Izquierdo-Garcia, P., Buendia, M., Filippone, S. & Martin, N. Synthetic chiral molecular nanographenes: the key figure of the racemization barrier. *Chem. Commun.* **58**, 2634–2645 (2022).
22. Shen, C. et al. Oxidative cyclo-rearrangement of helicenes into chiral nanographenes. *Nat. Commun.* **12**, 2786 (2021).
23. Evans, P. J. et al. Synthesis of a helical bilayer nanographene. *Angew. Chem. Int. Ed. Engl.* **57**, 6774–6779 (2018).
24. Dubey, R. K., Melle-Franco, M. & Mateo-Alonso, A. Inducing single-handed helicity in a twisted molecular nanoribbon. *J. Am. Chem. Soc.* **144**, 2765–2774 (2022).
25. Coquerel, Y. Aryne atropisomers: chiral arynes for the enantiospecific synthesis of atropisomers and nanographene atropisomers. *Acc. Chem. Res.* **56**, 86–94 (2023).
26. Kuck, D. Three-dimensional hydrocarbon cores based on multiply fused cyclopentane and indane units: centropolyindanes. *Chem. Rev.* **106**, 4885–4925 (2006).
27. Kuck, D. Benzoanellated centropolyquinanes, 15. Benzoanellated fenestranes with [5.5.5], [5.5.5.6], and [5.5.5.5] frameworks: the route from 1,3-indandione to fenestrindan. *Chem. Ber.* **127**, 409–425 (1994).
28. Khodaei, M. M. & Nazari, E. Synthesis of diarylmethanes via a Friedel–Crafts benzylation using arenes and benzyl alcohols in the presence of triphenylphosphine ditriflate. *Tetrahedron Lett.* **53**, 5131–5135 (2012).
29. Li, D. R., He, A. & Falck, J. R. Enantioselective, organocatalytic reduction of ketones using bifunctional thiourea-amine catalysts. *Org. Lett.* **12**, 1756–1759 (2010).
30. Noyori, R., Tomino, I. & Tanimoto, Y. Virtually complete enantioface differentiation in carbonyl group reduction by a complex aluminum hydride reagent. *J. Am. Chem. Soc.* **101**, 3129–3131 (1979).
31. Yamada, T. et al. Enantioselective borohydride reduction catalyzed by optically active cobalt complexes. *Chem. Eur. J.* **9**, 4485–4509 (2003).
32. Noyori, R. & Hashiguchi, S. Asymmetric transfer hydrogenation catalyzed by chiral ruthenium complexes. *Acc. Chem. Res.* **30**, 97–102 (1997).
33. Corey, E. J. & Helal, C. J. Reduction of carbonyl compounds with chiral oxazaborolidine catalysts: a new paradigm for enantioselective catalysis and a powerful new synthetic method. *Angew. Chem. Int. Ed. Engl.* **37**, 1986–2012 (1998).
34. Helal, C. J. & Meyer, M. P. in *Lewis Base Catalysis in Organic Synthesis* (eds Vedejs, E & Denmark, S. E.) 387–456 (Wiley, 2016).
35. Pronin, S. V., Reiher, C. A. & Shenvi, R. A. Stereoinversion of tertiary alcohols to tertiary-alkyl isonitriles and amines. *Nature* **501**, 195–199 (2013).
36. Bunrit, A. et al. Bronsted acid-catalyzed intramolecular nucleophilic substitution of the hydroxyl group in stereogenic alcohols with chirality transfer. *J. Am. Chem. Soc.* **137**, 4646–4649 (2015).
37. Roggen, M. & Carreira, E. M. Stereospecific substitution of allylic alcohols to give optically active primary allylic amines: unique reactivity of a (P,alkene)Ir complex modulated by iodide. *J. Am. Chem. Soc.* **132**, 11917–11919 (2010).
38. Rios, R. Enantioselective methodologies for the synthesis of spiro compounds. *Chem. Soc. Rev.* **41**, 1060–1074 (2012).
39. Vij, V., Bhalla, V. & Kumar, M. Hexaarylbenzene: evolution of properties and applications of multitalented scaffold. *Chem. Rev.* **116**, 9565–9627 (2016).
40. Yamano, R., Shibata, Y. & Tanaka, K. Synthesis of single and double dibenzohelicenes by rhodium-catalyzed intramolecular [2+2+2] and [2+1+2+1] cycloaddition. *Chem. Eur. J.* **24**, 6364–6370 (2018).
41. Mori, T. Chiroptical properties of symmetric double, triple, and multiple helicenes. *Chem. Rev.* **121**, 2373–2412 (2021).
42. Tanaka, H. et al. Symmetry-based rational design for boosting chiroptical responses. *Commun. Chem.* **1**, 38 (2018).
43. Cei, M., Di Bari, L. & Zinna, F. Circularly polarized luminescence of helicenes: a data-informed insight. *Chirality* **35**, 192–210 (2023).
44. Arrico, L., Di Bari, L. & Zinna, F. Quantifying the overall efficiency of circularly polarized emitters. *Chem. Eur. J.* **27**, 2920–2934 (2021).
45. Qiu, Z. et al. Amplification of dissymmetry factors in π-extended [7]- and [9]helicenes. *J. Am. Chem. Soc.* **143**, 4661–4667 (2021).
46. Nagata, Y. & Mori, T. Irreverent nature of dissymmetry factor and quantum yield in circularly polarized luminescence of small organic molecules. *Front. Chem.* **8**, 448 (2020).
47. Miguez-Lago, S. et al. Highly contorted superhelicene hits near-infrared circularly polarized luminescence. *Chem. Sci.* **13**, 10267–10272 (2022).
48. Ju, Y. Y. et al. Helical trilayer nanographenes with tunable interlayer overlaps. *J. Am. Chem. Soc.* **145**, 2815–2821 (2023).


## Acknowledgements

M.B., S.F., J.M.F.-G. and N.M. acknowledge financial support from the Spanish MICIN (project PID2020-114653RB-I00), they also acknowledge financial support from the ERC (SyG TOMATTO ERC-2020-951224) and from the '(MAD2D-CM)-UCM' project funded by Comunidad de Madrid, by the Recovery, Transformation and Resilience Plan and by NextGenerationEU from the European Union. M.B. also acknowledges financial support from the Spanish MICIN (project CTQ2017-83531-R). J.P. thanks M. Ramírez and P. Martínez-Martín for their help with the molecular models. We also acknowledge L. Favereau for his help in the CPL measurements at Rennes Institute of Chemical Sciences, Rennes, France.

## Author contributions

M.B., S.F., J.M.F.-G. and N.M. conceived and designed the experiments. M.B. performed the synthetic experiments and analysed data for all compounds. J.P. performed the X-ray crystallography. J.P., S.F. and N.M. co-wrote the paper.

## Competing interests
The authors declare no competing interests.

## Additional information
**Supplementary information** The online version contains supplementary material available at https://doi.org/10.1038/s44160-024-00484-x.

**Correspondence and requests for materials** should be addressed to Salvatore Filippone or Nazario Martín.

**Peer review information** *Nature Synthesis* thanks Yoann Coquerel and the other, anonymous, reviewer(s) for their contribution to the peer review of this work. Primary Handling Editor: Alison Stoddart, in collaboration with the *Nature Synthesis* team.